Deformation of Elastomeric Ethylene−Octene Copolymers

S. Bensason,[†] E. V. Stepanov,[†] S. Chum,[‡] A. Hiltner,*[,†] and E. Baer[†]

Department of Macromolecular Science and Center for Applied Polymer Research, Case Western Reserve University, Cleveland, Ohio 44106, and Polyolefins and Elastomers Research, The Dow Chemical Company, Freeport, Texas 77541

Received November 15, 1996; Revised Manuscript Received February 5, 1997[⊗]

ABSTRACT: The elastomeric behavior of low-crystallinity ethylene−octene copolymers prepared by Dow's INSITE constrained geometry catalyst technology is described. Deformation in uniaxial tension was examined as a function of comonomer content and molecular weight. Within the melting range of copolymers, temperature was used as an experimental variable to reveal the relationship between crystallinity and stress response. The concept of a network of flexible chains with fringed micellar crystals serving as the multifunctional junctions provided the structural basis for analysis of the elastic behavior. The rubber modulus scaled with crystallinity. Furthermore, the dimension of the fringed micellar junction obtained from the modulus correlated well with the average crystallizable sequence length of the copolymer. Because classical rubber theory could not account for the large strain dependence of the modulus, a theory which incorporates the contribution of entanglements to the network response was considered. Slip-link theory described the entire stress−strain curve. The slip-link density correlated with crystallinity; the cross-link density did not depend on crystallinity and appeared to represent a permanent network. The latter was further revealed by the effect of molecular weight on the stress−strain behavior. It is proposed that lateral attachment and detachment of crystallizable chain segments at the crystal edges provide the sliding topological constraint attributed to slip-links, and entanglements that tighten into rigid knots upon stretching function as permanent network junctions.

Introduction

Recent catalyst developments make available copolymers of ethylene with α-olefins that differ significantly from conventional LLDPEs.[1,2] In contrast to the broad comonomer and molecular weight distributions of LLDPEs synthesized with multisite catalysts,[3] the new copolymers are characterized by narrow molecular weight distribution, homogeneous comonomer distribution, and long chain branching structure. These features make the new copolymers excellent vehicles for fundamental studies of structure−property relationships in ethylene copolymers and other semicrystalline polymers.

Systematic correlations of copolymer composition with crystallinity, morphology, and tensile stress−strain behavior have been obtained using copolymers prepared by Dow's INSITE constrained geometry catalyst (CGCT) and process technology.[4,5] A composition of about 7 mol % octene comonomer (approximately 30% crystallinity) marks a gradual transition in the solid-state structure, characterized by a loss of spherulitic texture and a change in crystal morphology from lamellar to fringed micellar.[4] The transition occurs as random incorporation of increasing amounts of the noncocrystallizable comonomer gradually reduces the length of the crystallizable ethylene sequences. When the comonomer content is high enough, the crystallizable sequences are not long enough to chain fold into lamellar crystals. In the absence of chain folding, the crystallizable sequence length dictates the crystal thickness;[6] the lateral dimensions are restricted by crowding at the crystal−amorphous interface.[7]

The fringed micellar crystal was first proposed for semicrystalline homopolymers.[8,9] Although it was determined that these polymers crystallize from the melt as lamellae, the fringed micellar model may apply to crystallization from the glassy state.[10] The fringed micelle concept is particularly relevant to polymer chains with limited crystallizable sequence lengths. Examples include homopolymers with crystallizable stereoregular sequences such as PVC,[11] low-crystallinity ethylene−propylene copolymers,[12] ethylene−vinyl acetate copolymers, thermoreversible gels of crystallizable homopolymers and copolymers,[13] and segmented block copolymers such as thermoplastic polyurethanes.[14] A single polymer molecule will contain many sequences that are long enough to crystallize; these can be incorporated into different crystals to form a network of noncrystalline chain segments with fringed micellar crystals serving as the multifunctional junctions. The concept of a network of flexible chains anchored by thermally reversible, noncovalent junctions of high functionality provides the structural basis for the elasticity of thermoplastic elastomers.[15]

This concept may also be applicable to deformation of low−crystallinity CGCT copolymers. With the transition from lamellar to fringed micellar morphology, the stress−strain behavior of CGCT copolymers changes from yielding with necking to uniform extension. These low-density copolymers (0.86−0.88 g/cm^3) exhibit elastomeric behavior at ambient temperatures. Experimentally, the network structure is systematically varied in three ways: by changing the comonomer content, by changing the molecular weight, and by changing the temperature in the melting range. Analysis of the elastomeric behavior is approached with theories developed for cross-linked rubbers. Conventional rubber theory is used as an initial approach for validation of the hypothesis of a physical network built on fringed micellar crystal junctions. The more advanced slip-link theory[16,17] is used to analyze the entire stress−strain curve and to determine the role of the crystal junctions in elastomeric properties of CGCT copolymers.

Materials and Methods

Materials. Characteristics of the ethylene−octene elastomers produced by the INSITE constrained geometry catalyst technology are listed in Table 1. Copolymers in Table 1a vary

* To whom correspondence should be addressed.
[†] Case Western Reserve University.
[‡] The Dow Chemical Co.
[⊗] Abstract published in *Advance ACS Abstracts,* April 1, 1997.

S0024-9297(96)01685-3 CCC: $14.00

Table 1. Characteristics of Elastomeric CGCT Ethylene−Octene Copolymers

(a) Comonomer Content Variable

polym desig	mol % comonomer	melt index (g/10 min)	density[a] (g/cm^3)	density crystallinity (%)	heat of melting[b] (J/g)	DSC crystallinity (%)
CGCT88	8.2	0.9	0.8883	23	55	19
CGCT87	12.3	0.8	0.8730	12	36	12
CGCT86	13.6	0.5	0.8679	9	27	9

(b) Molecular Weight Variable

polym desig	M_w	M_n	melt index (g/10 min)	density[a] (g/cm^3)	density crystallinity (%)	heat of melting[b] (J/g)	DSC crystallinity (%)
CGCT87−57K	131700[c]	56700[c]	0.8	0.8730	12	36	12
CGCT87−37K	81700	37300	5	0.8757	14	36	12
CGCT87−32K	68600	32000	10	0.8747	14	37	13
CGCT87−26K	52300	26000	30	0.8751	14	32	11
CGCT87−20K	40200	19700	73	0.8763	15	41	14

[a] Measured from compression-molded plaques quenched into ice water [b] First-heating endotherms. [c] Extrapolated from the log−log relationship between melt index and molecular weight.

in branch content and have similar molecular weights, while copolymers in Table 1b have different molecular weights but similar branch content. The density of the compression-molded plaques was measured in a 2-propanol−water density gradient column calibrated with glass floats. Density crystallinity was calculated using a two-phase model with 0.855 g/cm^3 for the amorphous phase and 1.000 g/cm^3 for the crystalline phase. Thermal analysis experiments were carried out with a Perkin-Elmer Model 7 DSC. Percent crystallinity was calculated from first-heating scans at 10 °C/min based on a heat of fusion of 290 J/g for perfect crystals. Molecular weights measured by GPC and melt index values were provided by The Dow Chemical Co.

Methods. Materials were compression-molded at 190 °C and subsequently quenched in ice water, using conditions described previously.[4] Uniaxial tension measurements were obtained with 1.5 mm thick ASTM 1708 microtensile specimens cut from the compression-molded plaques. Specimens were stretched in an Instron 1123 testing machine with a crosshead speed of 22.25 mm/min, equivalent to an engineering strain rate of 1 min^{-1}, unless noted otherwise. Experiments at temperatures other than ambient were carried out in an environmental chamber. Specimens were equilibrated for 10 min at temperature before testing. Engineering stress was defined conventionally as force per initial cross-sectional area.

For measurement of strain, a pattern was coated on specimens by depositing 200 Å of gold over a square grid with 25 wires per in. Strain was measured midway along the specimen and was reported as extension ratio, defined as the deformed length of the square grid divided by the initial length. Because the specimens had a dumbbell shape, the varying cross-section in the fillet region led to some nonuniformity in deformation. In some cases, the strain distribution along the specimen during deformation was obtained from the grid pattern. Specimen deformation to fracture was recorded at 15× magnification by a video camera with a telescopic lens attachment. The maximum error in extension ratio was about ±0.1 in absolute scale. Data points on the stress−strain curves were picked from continuous data.

Results and Discussion

Experimental Results. Stress−strain curves for three copolymers at room temperature are presented in Figure 1. Similarities to the behavior of a conventional rubber, specifically uniform deformation to high strain and recovery following fracture, illustrate the elastomeric character of these copolymers at room temperature. The stress response at all strains increased with decreasing branch concentration as apparent in the initial modulus, the stress at intermediate strains, and the stress upswing at high strains. Because crystallinity increases as branching decreases, the observed trend suggests a structural correlation between crystallinity and stress response.

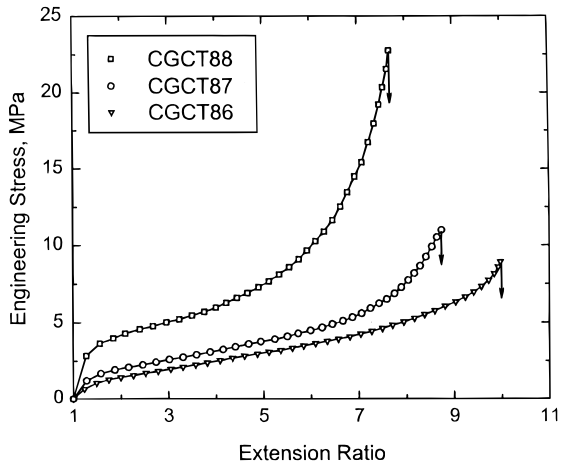

Figure 1. Stress−strain curves of three elastomeric CGCT copolymers at room temperature.

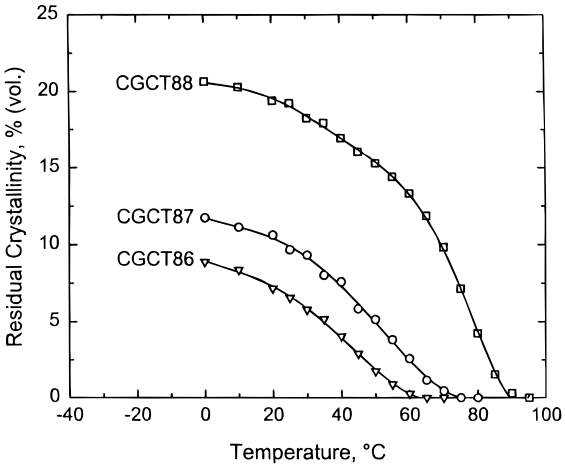

Figure 2. Volume crystallinity as a function of temperature in the melting range.

The relationship between crystallinity and deformation was further examined by changing the temperature within the melting range to vary crystallinity. The elastomeric ethylene−octene copolymers have low crystallinity and a broad melting range. Figure 2 shows the temperature dependence of the crystallinity for the three elastomers as reported in a previous study.[5] The crystallinity at 0 °C is 21, 12, and 9% (vol) for CGCT88, CGCT87, and CGCT86, respectively. Melting begins at subambient temperatures and crystallinity gradually

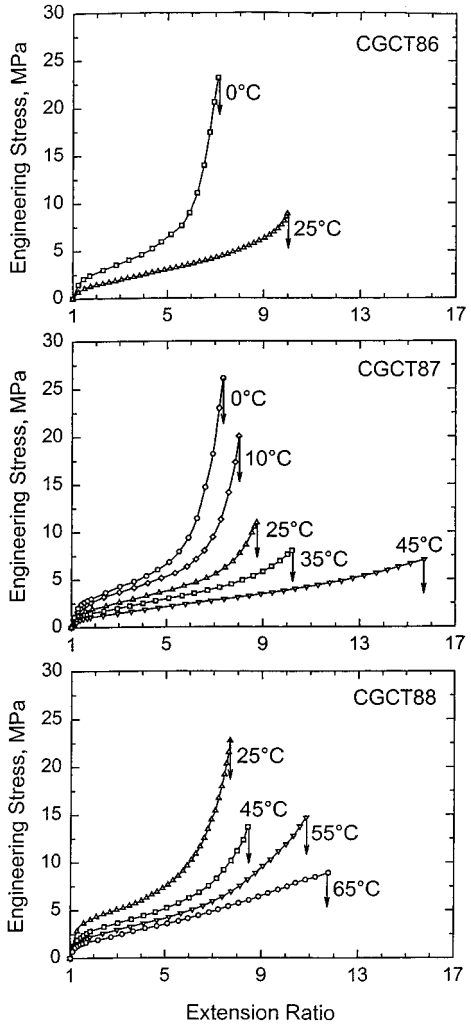

Figure 3. Stress−strain curves of elastomeric CGCT copolymers at various temperatures: (a) CGCT86; (b) CGCT87; (c) CGCT88.

decreases until melting is complete between 75 and 95 °C depending on the comonomer content.

The effect of temperature on deformation behavior of the three copolymers is shown in Figure 3a−c. As in room temperature experiments, deformation was uniform at all temperatures. With increasing temperature stress at all strains decreased and the fracture strain increased. Increasing temperature had a similar effect as increasing branching; both resulted in reduced crystallinity. Because there was no significant change in crystallinity below 0 °C and also to avoid temperatures close to the β-transition temperature,[4] no experiments were performed below 0 °C.

The effect of strain rate on deformation of CGCT87 at room temperature is presented in Figure 4. The data are expressed in terms of modulus G as it is usually defined for elastomers:[18]

$$G = \sigma/(\lambda - 1/\lambda^2) \tag{1}$$

where λ is the extension ratio and σ is the engineering stress. In all cases, a gradually decreasing modulus at low strains was followed by an upswing at high strains. The effect of strain rate was most pronounced at low strains. However, even in this region, the modulus changed by no more than 40% over four decades in strain rate. An intermediate strain rate of 1 min^{-1} was used in all other experiments.

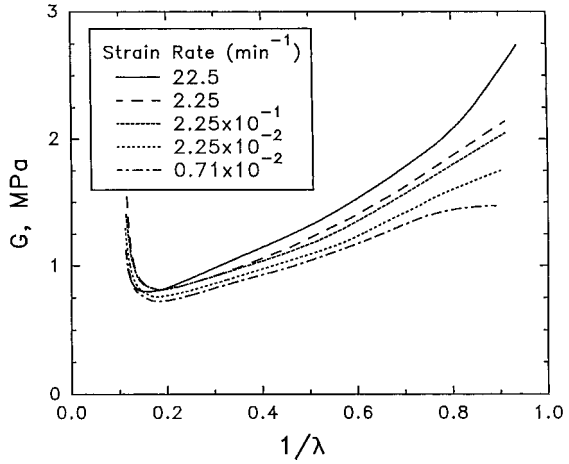

Figure 4. Effect of strain rate on the modulus of CGCT87 at room temperature.

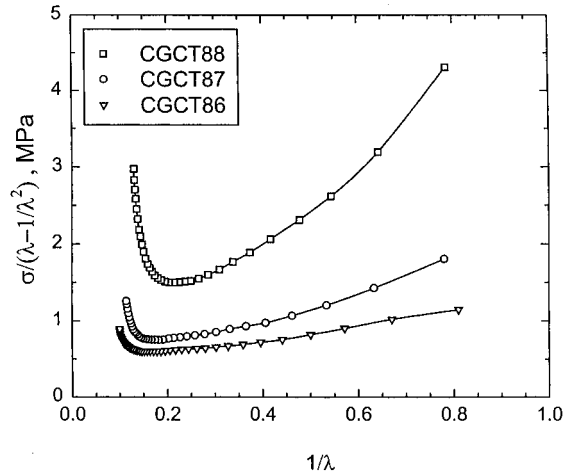

Figure 5. Modulus of three elastomeric CGCT copolymers at room temperature.

Interpretation by Classical Rubber Theory. The negligible effect of strain rate on the elastic modulus allows us to ascribe the response to deformation to the entropic elasticity of noncrystalline regions. In the absence of chemical cross-links, a physical network built on fringed micellar crystal junctions and perhaps entanglements was invoked to account for the elastomeric response. To test the relationship between structural features and deformation behavior, we use an analysis similar to the conventional treatment of the modulus of semicrystalline polymers,[19,20] however, taking into account features specific to micellar crystal junctions. Thus the modulus G is proportional to ν, the number of effective network chains per unit volume:

$$G = \nu kT \tag{2}$$

where k is the Boltzmann constant and T is the absolute temperature. Since crystallinity is low, here we can neglect the "filler" effect of crystallites. Data for the three copolymers at room temperature in Figure 5 indicate a gradually decreasing modulus at low strains, followed by an upswing at higher strains. The magnitude of both the modulus drop at low strains and the upswing at high strains increased with crystallinity. Qualitatively, the same kind of variation in G with extension is also typical for chemically cross-linked rubbers.[21]

Although the modulus is not independent of strain as required by the theory, it is possible to derive certain

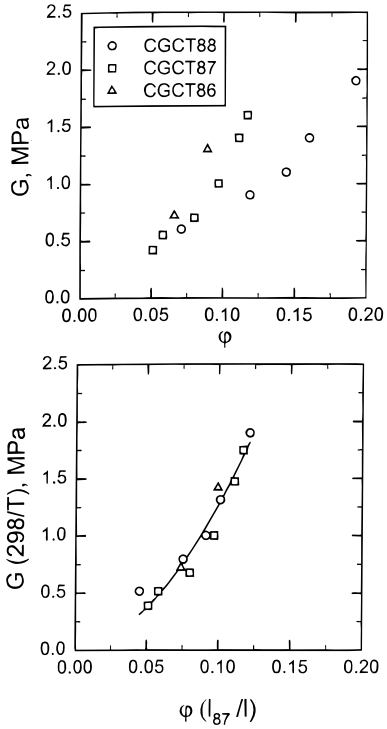

Figure 6. Relationship between modulus and crystallinity: (a) modulus at $\lambda = 2.5$ versus volume fraction crystallinity; (b) normalized modulus versus crystallinity normalized by the average chain length between branches.

structural characteristics of the network by examining the dependence of G on crystallinity. The quantity ν can be estimated from the structural model if total crystallinity and crystal size are known. The volume fraction of fringed micellar crystals ϕ may be expressed as

$$\phi = N(faL) \tag{3}$$

where N is the number of crystals per unit volume, f is the number of chains traversing the crystalline junction, a is the cross-sectional area per chain (18.7 Å^2 for polyethylene[22]), and L is the length of the crystal. Assuming that every chain terminates in two different crystals, the number of network chains that contribute to the modulus per unit volume is $\nu = Nf$. Hence, combining eqs 2 and 3

$$G = \phi kT/aL \tag{4}$$

It follows from eq 4 that the modulus should be proportional to the crystallinity normalized by crystal thickness L.

Modulus values at $\lambda = 2.5$, a strain where the effect of strain rate was minimal, were picked to examine the relationship between modulus and crystallinity (Figure 6a). Different crystallinities were obtained for each copolymer by varying the temperature. The dependence of modulus on crystallinity was different for each copolymer. To test for a relationship between G and ϕ based on the number of network chains, i.e. eq 4, data should be presented as (GT_0/T) vs $(\phi L_0/L)$, where T_0 and L_0 are a reference temperature and reference crystal length, respectively. Because the spacing between branches dictates the crystal thickness, proportionality is assumed between crystal length L and average crystallizable sequence length l for each copolymer. Then the ratio (L_0/L) can be replaced by (l_0/l). The average chain length between hexyl branches for CGCT86 with 13.6 mol % is 17 Å with the methylene groups in the all-trans configuration. For CGCT87 and CGCT88, the length is 19 and 30 Å, respectively. The normalized plot is shown in Figure 6b with CGCT87 ($l_0 = l_{87} = 19$ Å) at room temperature ($T_0 = 298$ K) as the reference. The differences among materials are largely removed and a single relationship between modulus and crystallinity, independent of temperature and crystal length, encompasses all the data. Nonlinearity in the relationship between reduced modulus and crystallinity may indicate that the crystal length L is not independent of temperature, which would violate the assumed proportionality between l and L. If this were the case, the crystal length for CGCT87 as calculated from eq 4 would vary from 25 Å at 45°C to 15 Å at 0 °C. Despite this variation, the calculated L values are in the same range as the crystallizable sequence length l.

Interpretation by Slip-Link Theory. To further explore the relationship between structure and deformation, more advanced theories of rubber elasticity were considered. The slip-link theory is based on reptation concepts and describes the elasticity of a cross-linked network by considering the additional contributions of entanglements[16] and finite chain extensibility[17] to the elastic free energy. Entanglements are visualized as slipping links that can slide along the chain contour between cross-links. The theory satisfactorily describes the variation of modulus with strain in cross-linked rubbers.[23]

The slip-link theory operates with four parameters: The density of cross-linked chains N_c, the density of slip-links N_s, the slippage parameter η, and the inextensibility parameter α. Slippage allows for the decreasing modulus at low strains and the parameter α describes the stress upswing at high strains. The free energy F derived from slip-link theory has the form

$$\frac{F}{kT} = \frac{1}{2}N_s\left(\sum_i\left[\frac{\lambda_i^2(1-\alpha^2)(1+\eta)}{(1-\alpha^2\sum_i\lambda_i^2)(1+\eta\lambda_i^2)} + \log(1+\eta\lambda_i^2)\right] + \log(1-\alpha^2\sum_i\lambda_i^2)\right) + \frac{1}{2}N_c\left(\frac{\sum_i\lambda_i^2(1-\alpha^2)}{(1-\alpha^2\sum_i\lambda_i^2)} + \log(1-\alpha^2\sum_i\lambda_i^2)\right) \tag{5}$$

where summation is performed over the three Cartesian components of strain λ. Stress in uniaxial tension is then obtained from eq 5 by

$$\sigma = \left(\frac{\partial F}{\partial \lambda}\right)_{T,V} \tag{6}$$

with $\lambda_1 = \lambda$ and $\lambda_2 = \lambda_3 = 1/\lambda^{1/2}$. If $\eta = 0$ the slip-links are rigid and act as crosslinks. For $\alpha = 0$, the cross-link term reduces to the classical theory of phantom chains.

Data fit was carried out with η held constant at 1.1, the value reported for cross-linked polyethylene filaments stretched in the melt state.[24] Initially, the stress upswing region was ignored by setting $\alpha = 0$, and initial

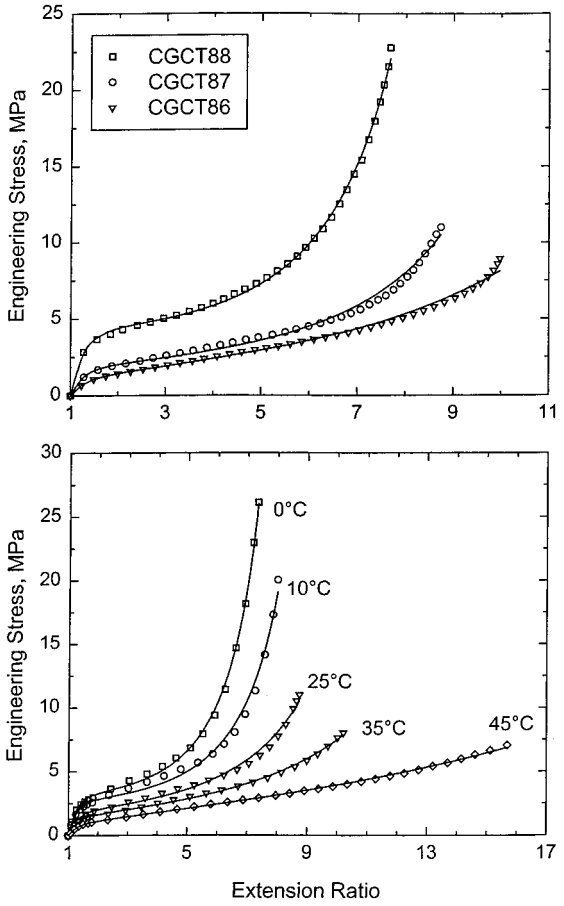

Figure 7. Comparison of stress−strain curves calculated from slip-link theory (solid lines) with experimental results (data points): (a) three CGCT copolymers at room temperature: (b) CGCT87 at various temperatures.

values N_c and N_s were determined. A three-parameter least-squares fit was subsequently performed to obtain α and final values of N_s and N_c. The calculated stress−strain curves, shown in Figure 7a,b, fit the entire range of deformation remarkably well.

The temperature dependence of the separate contributions of cross-links and slip-links to the total stress response of CGCT87 is shown in Figure 8a,b. At low strains the cross-link contribution is essentially unaffected by inextensibility and the behavior is similar to the prediction of the rubber theory. The slip-link contribution has a significantly different form when compared to cross-links and dominates the total stress at low strains. The initially high slip-link modulus decreases strongly at low strains as the links become free enough to slip. At about a draw ratio of 2 a yieldlike plateau is reached; the plateau stress depends on the number of slip-links. Cross-links contribute to the slope of the stress−strain curve at intermediate strains. Slip-links and cross-links make similar contibutions to the stress upswing at high strains because the inextensibility is incorporated into both slip-link and cross-link terms in eq 5 in the same manner. Unlike the cross-link contribution, which is independent of temperature at low and intermediate strains, the slip-link contribution does depend on crystallinity, and increasing crystallinity results in a larger plateau stress.

The parameters obtained from fits with $\eta = 1.1$ are shown in Table 2. The cross-link contribution is almost independent of density and temperature, and hence crystallinity, with a value of 0.35 ± 0.08 MPa. The slip-link density is larger than the crosslink density by at

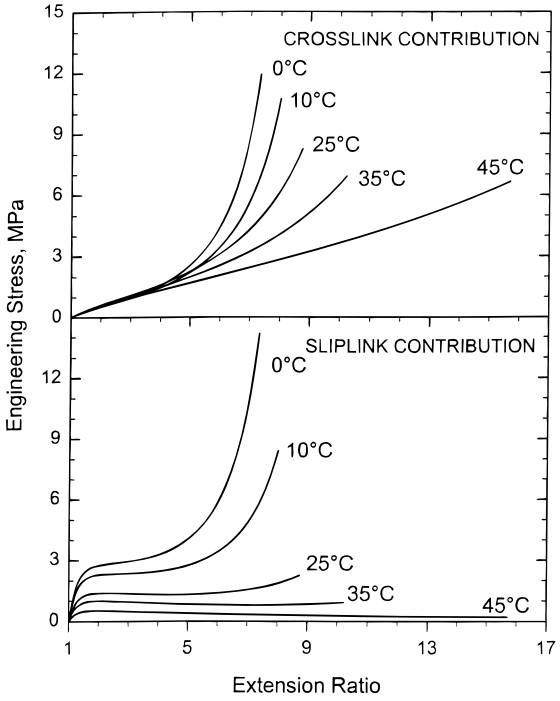

Figure 8. Separate contributions of cross-links and slip-links to the stress−strain curve: (a) cross-link contribution; (b) slip-link contribution.

Table 2. Slip-Link Parameters for Three Elastomeric Copolymers

temp (°C)	$N_c kT$ (MPa)	$N_s kT$ (MPa)	α
	CGCT86		
0	0.28	9.7	0.109
25	0.42	4.1	0.051
	CGCT87		
0	0.27	14.3	0.105
10	0.28	12.5	0.092
25	0.35	8.1	0.072
35	0.35	6.2	0.052
45	0.33	3.4	0.022
	CGCT88		
25	0.36	20.1	0.092
45	0.43	11.7	0.074
55	0.42	10.4	0.060
65	0.38	7.3	0.038

least an order of magnitude and depends on crystallinity. Comparing copolymers at room temperature, N_skT decreases with branch content; and for each copolymer, it decreases with temperature. As shown in Figure 9, the slip-link modulus N_skT correlates with crystallinity in the same way as G in Figure 6 and scales with l (crystallizable sequence length). The inextensibility parameter α increases with crystallinity and follows the same trends as slip-link density in each case.

Identification of crystals as slip-links can be readily visualized by considering the morphological features of the bundle-like crystals. Because the crystal dimensions are restricted along the chain direction due to noncrystallizable co-units, crystal formation and growth occur by lateral attachment of segments. Such crystal formation allows the surface chains to detach and, conversely, chains in the vicinity of the crystal surface to attach. This speculation leads to a situation schematically depicted in Figure 10, where a chain is anchored by its ends to two crystals, and in between a chain segment is attached to another crystal. Detachment of this crystallizable chain segment and subsequent reattachment of another crystallizable chain

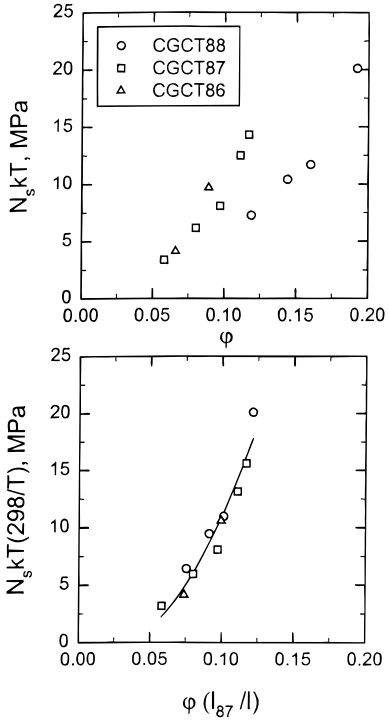

Figure 9. Relationship between slip-link modulus and crystallinity: (a) slip-link modulus versus volume fraction crystallinity; (b) normalized slip-link modulus versus crystallinity normalized by the average chain length between branches.

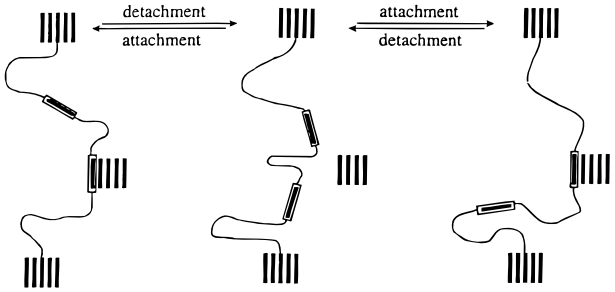

Figure 10. Schematic representation of detachment−attachment of crystallizable chain segments to produce a topological constraint equivalent to a slip-link.

segment result in a repartitioning of the network chains, which in effect is the same as slippage of a topological constraint along the chain contour.

The cross-links, on the other hand, should be visualized as junctions that remain rigid during stretching. Because their density does not change with temperature, and thereby does not correlate with crystallinity, their presence can only be treated as some type of topological constraint, i.e. entanglements. Indeed, at high strains, entanglements can tighten into knots that behave like rigid junctions. Therefore, the role of entanglements can change upon stretching. As described above, the effect of the cross-linked network on the elastomeric response is significant only at intermediate and high strains, and the calculated values of N_c are determined mainly by those parts of the stress−strain curves. At low strains, the entanglements certainly behave like slip-links; however, because $N_c \ll N_s$, this additional contribution to the net number of slip-links is not perceptible. Thus the interpretation of cross-links as entangled knots that tighten as strain increases seems to be reasonable.

Molecular Weight Effect. The effect of molecular weight on stress−strain behavior was investigated with

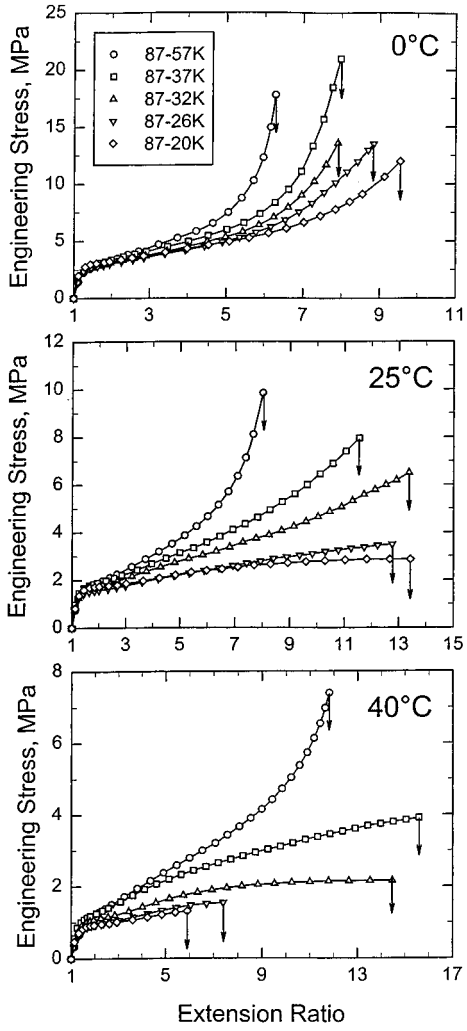

Figure 11. Stress−strain curves of CGCT87 copolymers of various molecular weights: (a) at 0 °C; (b) at 25 °C; (c) at 40 °C.

a set of ethylene−octene copolymers that had a density similar to that of CGCT87, yet differed in molecular weight. The effect of molecular weight on the stress−strain behavior at 0, 25, and 40 °C is shown in Figure 11a−c. The low-strain portion of the stress−strain curves, encompassing the tensile modulus region, was virtually identical for all molecular weights. Differences in stress response first became apparent at intermediate strains, above $\lambda = 2$, where decreasing molecular weight resulted in a lower slope. The salient features of the molecular weight effect on the stress−strain curve are in general agreement with observations for higher crystallinity ethylene copolymers.[25] The insensitivity of the low-strain region to molecular weight confirms that this region is primarily influenced by the degree of crystallinity, which is very similar for all the materials (Table 1).

The effect of molecular weight was most pronounced at large strains. A stress upswing, characterized by an increasing slope in the stress−strain curve, was observed for all materials at 0 °C. The strength of the upswing decreased with decreasing molecular weight and the strain at fracture increased. At 25 °C, the lower molecular weight polymers exhibited no stress upswing, yet a large strain at fracture. When the stress upswing was absent, a gradual decrease in slope was observed at draw ratios of 6 and higher, even though the stress continued to increase. At 40 °C all the polymers except

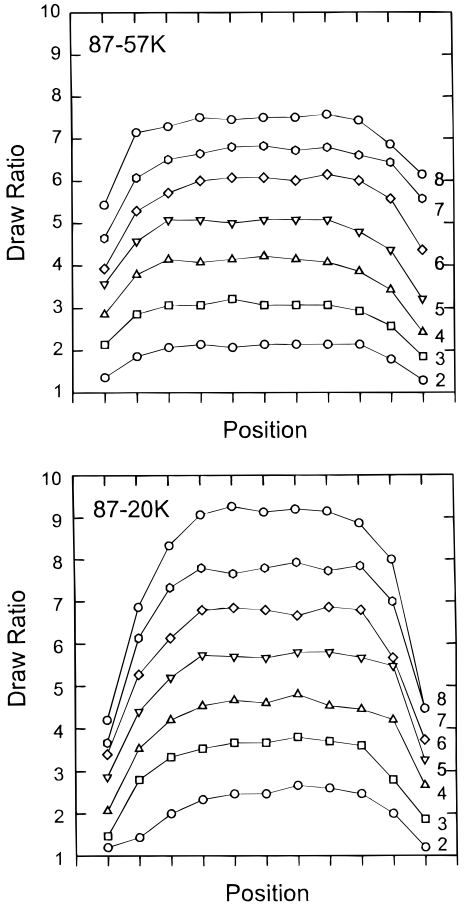

Figure 12. Strain distribution along the specimen at 35 °C measured at various remote strains: (a) CGCT87-57K; (b) CGCT87-20K.

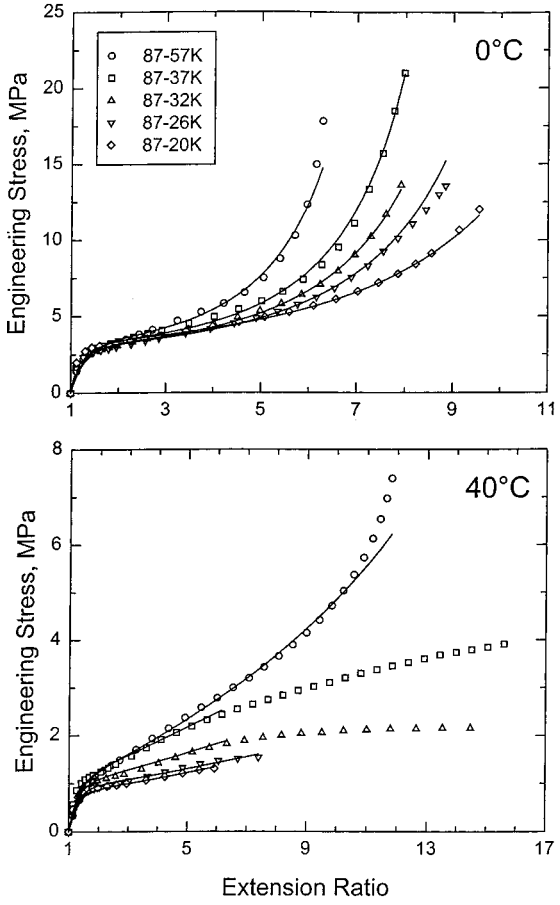

Figure 13. Comparison of stress−strain curves calculated from slip-link theory (solid lines) with experimental results (data points) for CGCT87 copolymers of various molecular weights: (a) at 0 °C; (b) at 40 °C.

CGCT87−57K exhibited a decreasing slope at high strains. The fracture strain decreased for CGCT87-26K and CGCT87-20K.

Associated with the decreasing slope in the stress−strain curve was a change in the strain distribution along the specimen. The variation of strain along specimens of CGCT87-20K and CGCT87-57K during deformation at 35 °C is illustrated in Figure 12. Numbers on the curves indicate the remote strain calculated from the initial separation of the grips. Figure 12 clearly reveals that the strain distribution was much broader in CGCT87-20K than in CGCT87-57K. A broad distribution of strain along the specimen accompanied all the stress−strain curves that exhibited a decrease in slope beyond a draw ratio of 6. The decreasing slope of the stress−strain curves at high strain may be interpreted as a breakdown in the network connectivity beyond a draw ratio of about 6. Indeed, the recovery following fracture observed for lower molecular weight copolymers was less than that observed for CGCT87-57K, consistent with a loss in network connectivity. Because the theories operate with intact networks, data for extension ratios exceeding 6 were omitted from the analysis when a decreasing slope was observed in the stress−strain curve.

Molecular weight data were analyzed by the slip-link theory. Fits to experimental data and the resultant fitting parameters are shown in Figure 13a−c and Table 3. The slip-link modulus was insensitive to variations in molecular weight. The deviation from the mean was not more than 10% at all temperatures. This supports the association of slip-links with crystallinity, since the

Table 3. Slip-Link Parameters for Copolymers of Various Molecular Weights

copolymer	0 °C	25 °C	35 °C	40 °C
	$N_s kT$ (MPa)			
CGCT87−57K	14.5	7.8	5.4	3.8
CGCT87−37K	15.0	7.0	5.5	4.3
CGCT87−32K	14.3	7.3	5.0	4.4
CGCT87−26K	14.2	7.1	5.1	4.3
CGCT87−20K	15.5	7.1	5.6	3.8
	$N_c kT$ (MPa)			
CGCT87−57K	0.29	0.35	0.39	0.36
CGCT87−37K	0.33	0.43	0.34	0.34
CGCT87−32K	0.36	0.36	0.28	0.23
CGCT87−26K	0.37	0.28	0.23	0.17
CGCT87−20K	0.40	0.28	0.19	0.16
	α			
CGCT87−57K	0.110	0.075	0.053	0.033
CGCT87−37K	0.091	0.036	0	0
CGCT87−32K	0.082	0.025	0	0
CGCT87−26K	0.075	0	0	0
CGCT87−20K	0.062	0	0	0

crystallinity of the materials did not vary significantly (Table 1b). In contrast, the cross-link modulus exhibited considerable variation as a function of molecular weight. The effect of N_c was apparent from the slope of the stress−strain curves at intermediate strains. Generally, $N_c kT$ increased with increasing molecular weight, except at 0 °C. The N_c values at 0 °C have to be interpreted in conjunction with the accompanying inextensibility parameter α because the upswing produced by a high inextensibility parameter overlaps with the cross-link contribution at intermediate strains. Hence, a comparison of cross-link modulus among molecular

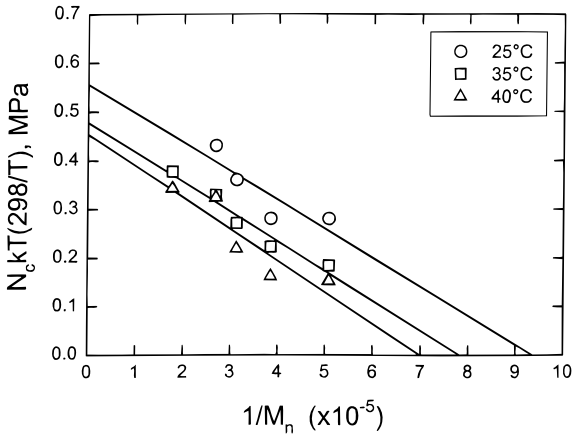

Figure 14. Dependence of the cross-link modulus on molecular weight of CGCT87.

Table 4. Critical Molecular Weight Calculated from N_c

temp (°C)	M_c (from *x*-intercept)	M_c (from *y*-intercept)
25	5330	3810
35	6390	4430
40	7150	4670

weight materials is best made when the inextensibility parameter is either small or zero. Thus, data at 0 °C and data for CGCT87-57K at 25 °C are omitted in the following analysis.

If cross-links are visualized as tightened entanglement knots, the interpretation of the molecular weight effect is analogous to that for chemically cross-linked rubbers. In this case, the effect of decreasing molecular weight is attributed to the increasing number of chain ends, which reduces the number of effective network chains.[26] By the analogy with rubber theory, the effective cross-link density N_c for tetrafunctional cross-links is characterized by the relationship

$$N_c = N_{c,o}(1 - 2M_c/M_n)$$

where $N_{c,o}$ is the cross-link density if all chains are effective (i.e. at infinite molecular weight), M_c is the critical molecular weight between junctions, and M_n is the number-average molecular weight. The term in parentheses indicates the fraction of chains that are effective, i.e. with both ends terminating at junctions. A plot of the cross-link modulus against reciprocal molecular weight (Figure 14) yields a linear relationship for each temperature. The critical molecular weight calculated from the *x*-intercept ranges from 5330 and 7150 and is listed in Table 4. Neglecting the small amount of crystallinity, $N_{c,o}$ can be estimated as $N_{c,o} \cong \rho/M_c$, where ρ is the density, and then M_c can also be obtained from the *y*-intercept of Figure 14. Results are listed in Table 4.

The fair agreement between the two estimates of critical molecular weight indicates that the effect of decreasing molecular weight is indeed similar to the effect that would be observed for a tetrafunctional network. The slight difference between the M_c estimates is usually ascribed to deviation of the chain end-to-end distance distribution from Gaussian. Furthermore, the values of M_c are of the order of magnitude with the critical molecular weight reported for entangled ethylene copolymer melts, about 3500−4000.[27,28] Hence the effect of molecular weight can be ascribed to the number of entanglements per chain in the network and suggests that the entanglements between fringed micellar crystals act like cross-links in a permanent network. This is also consistent with the trend of increasing M_c with temperature, because crystallinity provides some additional topological constraints near the crystal interface.

In summary, the slip-link theory describes the experimental data for elastomeric ethylene copolymers successfully. The response of the fringed micellar network to deformation has separate contributions from slipping links and rigid cross-links. Slip-links produce a high initial modulus that transforms to a plateau stress in a manner reminiscent of a yieldlike process. The cross-links are primarily effective at large strains and provide the slope of the stress−strain curve. Slip-link density correlates with crystallinity and is insensitive to variations in molecular weight. In contrast, the cross-link density is independent of crystallinity and depends on molecular weight. A structural interpretation of slipping links is proposed in light of the fringed micellar morphology. Lateral attachment and detachment of crystallizable chain segments at the crystal edges result in repartitioning of the chain contour length and have the same effect as sliding topological constraints. The cross-links are attributed to entanglements that tighten upon stretching. These interpretations differ from the structural features treated in the slip-link theory. Nevertheless, consideration of two types of links is a plausible approach to analyzing the elastomeric response of ethylene−octene copolymers. The next step is to build a theoretical framework for the elasticity that takes into account the specific structural details of a physical network built on fringed micellar crystals, such as a "slippage" borne by chains attaching−detaching to crystals and a "cross-linkage" due to tightened entanglements.

Acknowledgment. The authors gratefully recognize the contributions of Professor I. M. Ward in discussions of advanced rubber theories. This work was generously supported by The Dow Chemical Co.

References and Notes

(1) Sehanobish, K.; Patel, R. M.; Croft, B. A.; Chum, S. P.; Kao, C. I. *J. Appl. Polym. Sci.* **1994**, *51*, 887.
(2) Hwang, Y.-C.; Chum, S.; Guerra, R.; Sehanobish, K. In *ANTEC'93 SPE Conf. Proc.* **1993**, 1188.
(3) Wilfong, D. L.; Knight, G. W. *J. Polym. Sci., Part B: Polym. Phys.* **1990**, *28*, 861.
(4) Bensason, S.; Minick, J.; Moet, A.; Chum, S.; Hiltner, A.; Baer, E. *J. Polym. Sci., Part B: Polym. Phys.* **1996**, *34*, 1301.
(5) Minick, J.; Moet, A.; Chum, S.; Hiltner, A.; Baer, E. *J. Appl. Polym. Sci.* **1995**, *58*, 1371.
(6) Mathot, V. B. F. In *Calorimetry and Thermal Analysis of Polymers;* Mathot, V. B. F., Ed.; Hanser Publishers: New York, 1994; Chapter 9.
(7) Flory, P. J. *J. Am. Chem. Soc.* **1962**, *84*, 2857.
(8) Hermann, K.; Gengross, O. *Kautschuk* **1932**, *8*, 181.
(9) Bryant, W. M. D. *J. Polym. Sci.* **1947**, *2*, 547.
(10) Wunderlich, B. *Macromolecular Physics;* Academic Press: New York, **1976**; Vol. 2, Chapters 5, 6.
(11) Stephenson, R. C.; Smallwood, P. V. Vinyl Chloride Polymers/Structure and Properties. In *Encyclopedia of Polymer Science and Engineering*, 2nd ed.; Mark, H. F., Bikales, N. M., Overberger, C. G., Menges, G., Eds.; John Wiley & Sons: New York, 1985; Supplement Volume, p 847.
(12) Ver Strate, G. *Ethylene−Propylene Elastomers.* In *Encyclopedia of Polymer Science and Engineering*, 2nd ed.; Mark, H. F., Bikales, N. M., Overberger, C. G., Menges, G., Eds.; John Wiley & Sons: New York, 1985; Vol. 6, p 533.
(13) Guenet, J.-M. *Thermoreversible Gelation of Polymers and Biopolymers;* Academic Press: New York, 1992; Chapter 1.
(14) Cooper, S. L.; Tobolsky, A. V. *J. Appl. Polym. Sci.* **1966**, *10*, 1837.

(15) *Thermoplastic Elastomers: A Comprehensive Review;* Legge, N. R., Holden, G., Schroeder, H. E., Eds.; Hanser Publishers: New York, 1987.
(16) Ball, R. C.; Doi, M.; Edwards, S. F.; Warner, M. *Polymer* **1981**, *22*, 1010.
(17) Edwards, S. F.; Vilgis, Th. *Polymer* **1986**, *27*, 483.
(18) Treloar, L. R. G. *The Physics of Rubber Elasticity;* Oxford University Press: London, 1967.
(19) Nielsen, L. E.; Stockton, F. D. *J. Polym. Sci.* **1963**, *A1*, 1995.
(20) Krigbaum, W. R.; Roe, R.-J.; Smith, K. J., Jr. *Polymer* **1964**, *5*, 533.
(21) Mark, J. E. *Rubber Chem. Technol* **1975**, *48*, 495.
(22) Geil, P. H. *Polymer Single Crystals;* Wiley-Interscience: New York, 1963; Chapter 1.
(23) Thirion, P.; Weil, T. *Polymer* **1984**, *25*, 609.
(24) Brereton, M. G.; Klein, P. G. *Polymer* **1988**, *29*, 970.
(25) Kennedy, M. A.; Peacock, A. J.; Failla, M. D.; Lucas, J. C.; Mandelkern, L. *Macromolecules* **1995**, *28*, 1407.
(26) Flory, P. J. *Principles of Polymer Chemistry;* Cornell University Press: New York, 1953; Chapter 11.
(27) Seguela, R.; Rietsch, F. *J. Mater. Sci.* **1988**, *23*, 415.
(28) Graessley, W. W.; Edwards, S. F. *Polymer* **1981**, *22*, 1329.

MA961685J